

Relativistic particle incoherent scattering by the nuclei of crystal plane atoms

Victor V. Tikhomirov

*Research Institute for Nuclear Problems,
Belarusian State University, Minsk, Belarus*

(Dated: March 5, 2021)

Abstract

A consistent theory, which describes the incoherent scattering of classically moving relativistic particles by the nuclei of crystal planes without any phenomenological parameter is presented. The basic notions of quantum mechanics are applied to introduce a fundamental compact formula for the mean square incoherent scattering angle per unit length of particle trajectory. The latter is used to implement the effects of the crystal atom distribution inhomogeneity into the Coulomb scattering simulations without noticeable elongation of the simulation time. The theory essentially reconsiders the nature of positively charged particle dechanneling from the low nuclear density regions, being essential in both the crystal undulators and envisaged measurements of the specific electromagnetic momenta of short living particles.

PACS numbers: 61.85.+p,12.20.Ds

I. INTRODUCTION

When a fast particle is moving along a string or plane of atoms in a crystal, nanotube or other ordered structure, it experiences correlated collisions with successive atoms which result in the strong particle deflection described by an effective field [1] exceeding any created in laboratory by the orders of value [2–6]. Such strong fields provide a unique tool for the high energy particle beam manipulations, such as collimation [7–13], focusing [14–16], extraction [17–20]; hard narrow spectrum gamma-radiation, including coherent bremsstrahlung [4, 5, 21], string-of-string [22, 23], channeling [2, 4, 24], parametric [2, 25] and crystal undulator radiation [2, 26–32]; both the coherent [4, 5, 21] and synchrotron-like electron-positron pair production [3, 5, 6, 33]; quantum electrodynamic effects of both electron and positron magnetic moment modification [34, 35], vacuum dichroism, birefringence [2, 3, 5, 33] and some others [5, 6, 36]; production, manipulation and analysis of polarized gamma [2, 3, 5, 33] and electron/positron beams [23, 37–41]; the reduction of the thickness of particle detectors and making them sensitive to both direction and polarization as well as revealing the new factors which determine their energy resolution [42, 43], search and measurement of both magnetic and electric dipole as well as electric quadrupole momenta of short living particles [2, 37, 44–48], etc.

All the mentioned coherent effects experience an impact of the incoherent scattering. Though the latter has much in common with the scattering by isolated atom or atom in amorphous medium, observable modifications of relativistic particle incoherent scattering in crystals arise due to both the atom and electron distribution inhomogeneity in the impact parameter plane, characterized by the r.m.s. amplitude u_1 of atom thermal vibrations. The latter give rise to the large correlations of the small momentum transfers $q \leq \hbar/u_1$, which merge together into a smooth coherent scattering process, described by the Lindhard potential [1], ceasing to contribute to the mean square angle of incoherent scattering, the decrease of which is directly measurable.

Though the problem of the specific incoherent scattering in crystals has been known since 50-th [21, 57] and addressed by several authors [50–56], the difference of the incoherent scattering in crystals from the scattering in amorphous medium has been explicitly demonstrated only recently [59]. The experiment has been conducted at the incidence angles, large enough to simultaneously simplify the particle motion, scattering theory and reliable extraction of

the 7% root mean square angle reduction in a $30\mu\text{m}$ Si crystals. However, being obtained as an average over the straight-line particle trajectories with arbitrary impact parameters for the whole crystal, the measured value has given only an average scattering characteristic for a uniform particle flux. The latter, in general, differs from local scattering characteristics met by both negatively charged channeling particles inside the dense nuclear regions and positively charged ones far outside the latter. The newly available experiments [19, 20, 58] in electron deflection and radiation both need a quantitative theory of dechanneling of electrons and provide at the same time the abundant data for its verification. The problem of stable channeling of positively charged particles is related with the strong violation of the proportionality of incoherent scattering intensity to the local nuclear density [1, 49, 50], related to the sharp decrease of the latter, proceeding greatly ahead of the same of the fields of all the distant plane atoms, becoming the leading source of incoherent scattering.

To be both correct and practical, the theory of relativistic particle scattering has to combine the semiclassical scattering treatment [1] of particle motion in the averaged potential with the quantum one [64, 65] for its perturbation by a single atom potential. This problem has been already treated [50] using the Wigner function approach in the axial case. Though the latter is more general and symmetric, such promising applications as short living particle electromagnetic moment measurement, crystal undulator development, channeled electron beam radiation, extraction and focusing need the incoherent scattering theory in planar case. Contrary to the axial one, the latter allows for an explicit treatment of the particle transverse phase space using the 1D wave functions, making possible a more reliable approach to the incoherent scattering problem.

Being applied to the incoherent scattering problem, the Wigner function has to reduce to the phase space density, equal to the product of a local nuclear density by the differential scattering cross section, in the classical limit. However, the quantum evaluation demonstrates negative values, making it necessary to resort to the positively determined mean square scattering angles for the small momentum transfer simulations [50]. At the same time, the large momentum transfers need the modified Coulomb cross section for their simulation. To avoid introduction of the corresponding special value, one can combine the high momentum cross section correction with the low momentum mean square modification angle into a single additional term to the Coulomb logarithm.

The paper is organized as follows. The channeling particle wave function perturbation

by the incoherent scattering by a single atom is introduced in Section II. Along with the Coulomb scattering basics, quoted in Appendix A, the increase of the energy of transverse channeling motion, induced by the incoherent scattering, is used in Section III to extract the local mean square incoherent scattering angle per unit length, compared with the 2D theory of [50] in Appendix B. The effects of scattering modification at all the momentum transfers in the presence of the plane atom distribution inhomogeneity are represented in the form of a Coulomb scattering logarithm correction in Section IV. The specific nature of the qualitative modification of incoherent scattering in the low nuclear density regions is addressed in both Section IV and Appendix C.

II. A CHANNELING PERTURBATION BY A SINGLE ATOM

To be both correct and effective, the theory of incoherent particle scattering in inhomogeneous medium should combine the unremovable quantum treatment of single atom scattering [18, 64] with the classical picture of ultrarelativistic particle motion in the average potential [1, 2], essentially simplifying all the consideration at high energies. The most reliable way to introduce the latter correctly, is a grounded reduction of the basic quantum approach. To arrive to the mean square scattering angle of a classically moving particle, we will proceed from the average increment of the energy of transverse particle motion. Being, for instance, confident in the possibility to neglect the quantum features of transverse oscillatory channeling motion at high enough energies [1, 2], one can limit consideration to the particle incoherent scattering by a single atomic plane.

The exhaustive treatment of both the channeling and related phenomena [2] proceeds from the "squared" Dirac equation [60] (the system of units $c = \hbar = 1$ is used through the paper)

$$\left[\Delta + p^2 - 2\varepsilon U(\mathbf{r})\right] \Psi(\mathbf{r}) = 0, \quad (1)$$

in which ε and p are particle energy and momentum respectively, $\Psi(\mathbf{r})$ and $U(\mathbf{r})$ are particle wave function and potential energy (potential for short) at a point \mathbf{r} . Unperturbed planar channeling is described by the one-dimensional planar potential $U(x)$, in which the coordinate x is measured along the plane normal.

Most of the multiple channeling applications involve bent crystals, in which the effective planar potential becomes asymmetric and depends on the particle energy. At this, such

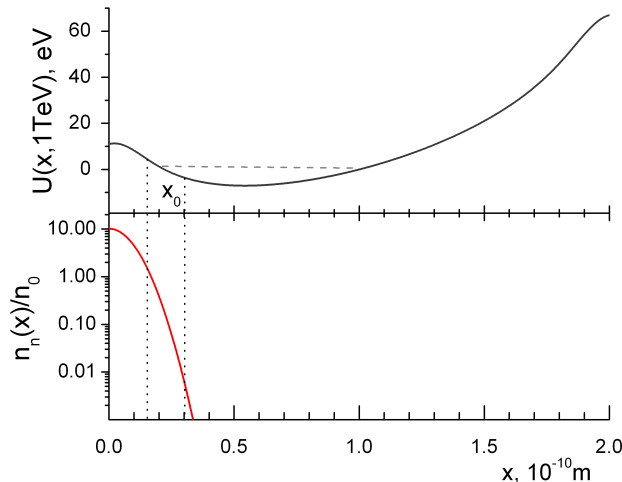


FIG. 1: The x -coordinate dependence of (110) Ge plane effective potential at 1 TeV particle energy, bent with 5 m radius (top), and the averaged planar nuclear density, measured in units of its average crystal value n_0 (bottom).

bent crystal applications as crystal undulators and measurements of short living particle specific electromagnetic momenta, reach their maximal efficiency at the extreme bending, illustrated by Fig. 1, which makes the dechanneling problem critical even for the most deeply channeled positively charged particles. Provided the nuclear density becomes negligible near the potential minima, the dechanneling theory describing the particle scattering by the thermal perturbations (singular phonons) of the atoms of the nearest crystal plane will be developed below mostly in view of these promising channeling applications.

The solution

$$\Psi(\mathbf{r}) = e^{ip_z z} \varphi(x) \quad (2)$$

of Eq.(1) with the planar potential $U(\mathbf{r}) = U(x)$ includes the wave function $\varphi(x)$ of transverse motion, which obeys the "relativistic Schrödinger equation"

$$\hat{H}_0 \varphi(x) = \left[\frac{\hat{p}_x^2}{2\varepsilon} + U(x) \right] \varphi(x) = \left[-\frac{1}{2\varepsilon} \frac{d^2}{dx^2} + U(x) \right] \varphi(x) = \varepsilon_n \varphi(x), \quad (3)$$

where $\hat{p} = -i\partial/\partial x$ and $\varepsilon_n = (p^2 - p_z^2)/2\varepsilon$ are the momentum operator and energy of the transverse motion.

Equation $U(x_0) = \varepsilon_n$ determines the classical turning point coordinate x_0 , see Fig. 1. Both the channeling stability and incoherent scattering theory issues reach the maximum

urgency in the region $x_0 = (2 \div 3)u_1 \sim 0.2 \text{ \AA}$ of the sharp decrease of the average nuclear density of an atomic plane

$$n_n(x_n) = n_0 d \frac{\exp(-x_n^2 u_1^2 / 2)}{\sqrt{2\pi} u_1}, \quad (4)$$

where n_0 and d are, respectively, the average crystal atomic density and inter-plane distance. Since the Gaussian (4) changes much faster than the average potential at $x_n \simeq x_0 \simeq (2 \div 3)u_1$, the linear approximation

$$U(x,.) \simeq \varepsilon_n + U'(x_0)(x - x_0) = \varepsilon_n - E(x_0)(x - x_0), \quad (5)$$

where $E(x_0) = -U'(x_0)/e$ is electric field strength at the turning point, can be readily applied for the latter, reducing Eq. (1) to

$$\left[\frac{d^2}{dx^2} + 2eE(x - x_0)\varepsilon \right] \varphi(x) = \left[\frac{d^2}{d\xi^2} - (\xi_0 - \xi) \right] \varphi(\xi) = 0, \quad (6)$$

$$\xi = \xi' x, \quad \xi_0 = \xi' x_0, \quad \xi' \equiv \frac{d\xi}{dx} = \sqrt[3]{2e|E|\varepsilon} = \text{const} > 0. \quad (7)$$

Eq. (6) solution [65]

$$\varphi(x - x_0) = \sqrt{\frac{2\pi\varepsilon}{\xi'}} Ai(\xi_0 - \xi) = \sqrt{\frac{\varepsilon}{2\pi\xi'}} \int_{-\infty}^{\infty} \exp[i(\xi_0 - \xi)t + it^3/3] dt \quad (8)$$

contains an Airy function Ai , which decreases sharply in the under-barrier $x < x_0$ and oscillates fast (see Fig. 18 in [3]) in the classical motion region $x > x_0$ at high particle energies. The solution (8) has been normalized according to the condition

$$\frac{dP(x)}{dx} = |\overline{\varphi(x - x_0)}|^2 = v^{-1}(x) \quad (9)$$

for the averaged transverse probability density, where

$$v(x) \simeq \sqrt{2e|E|(x - x_0)/\varepsilon} = \sqrt{(x - x_0)} \xi^{3/2} / \varepsilon \quad (10)$$

is the transverse particle velocity in the linearized potential (5). Such a normalization will simplify the introduction of the quantum scattering characteristics for a classically moving particle below.

An average value of the transverse energy increment, induced by the particle incoherent scattering, is readily evaluated through the Schrödinger equation of the transverse particle motion

$$i \frac{d\Psi}{dx} = \hat{H}\Psi, \quad \hat{H} = \hat{H}_0 + \delta U(x - x_n, y - y_n, z - z_n), \quad (11)$$

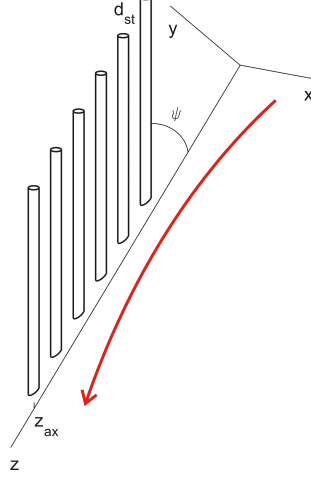


FIG. 2: Particle motion in the field of atomic strings (cylinders), constituting an atomic plane, parallel to yz coordinate plane. Planar channeling motion (thick red curve) occurs in xz plane, constituting a small angle $\psi \ll 1$ with the atomic strings, which form yz plane.

perturbed by the residual atomic potential [51, 52]

$$\delta U(\mathbf{r} - \mathbf{r}_n) = U_{at}(\mathbf{r} - \mathbf{r}_n) - \int \int U_{at}(\mathbf{r} - \mathbf{r}_n) n_n(x_n, y_n, z) dx_n dy_n, \quad (12)$$

where

$$U_{at}(\mathbf{r} - \mathbf{r}_n) = \frac{Z\alpha}{|\mathbf{r} - \mathbf{r}_n|} e^{-|\mathbf{r} - \mathbf{r}_n|\kappa} \quad (13)$$

is the screened atomic potential with the screening constant $\kappa = 1/r_{sc}$ and radius r_{sc} and

$$n_n(x_n, y_n, z) = \frac{1}{2\pi u_1^2 d_{at}} \exp \left\{ -x_n^2 u_1^2 / 2 - [y_n \cos \psi + (z - z_{ax}) \sin \psi]^2 u_1^2 / 2 \right\} \quad (14)$$

the atomic string nuclear density, characterized by both the atom thermal vibration amplitude u_1 and interatomic distance d_{at} , while z_{ax} is the coordinate of the string intersection with the plane xz of channeling oscillations. Though we consider the planar channeling, the string atomic structure inside a plane (see Fig. 2) should be taken into consideration to treat the incoherent scattering in both xz and yz planes adequately.

A substitution $\Psi(\mathbf{r}) = e^{ip_z z} f(\mathbf{r}) \varphi(x)$ introduces a wave function modification factor $f(\mathbf{r})$ which obeys the equation

$$i \frac{\partial f(\mathbf{r})}{\partial z} = \frac{\varepsilon}{p_z} \delta U(\mathbf{r} - \mathbf{r}_n) f(\mathbf{r}) - \frac{1}{p_z} \frac{\partial f(\mathbf{r})}{\partial x} \frac{d\varphi(x)}{dx} - \frac{1}{2p_z} \Delta_{\perp} f(\mathbf{r}) \simeq \frac{1}{v} \delta U(\mathbf{r} - \mathbf{r}_n) f(\mathbf{r}). \quad (15)$$

In general, both the full Eq. (15) and factor $f(\mathbf{r})$ describe both channeling and above-barrier motion of the particles scattered by an atom at various angles in a complex way. However

to treat the average transverse energy increase, one can consider only the right hand side limit of Eq. (15), resulting in the solution

$$f(x - x_n, y - y_n, z = z_n + 0) \simeq \exp\left(-i \int_{-\infty}^{\infty} \delta U(x - x_n, y - y_n, z) \frac{dz}{v}\right), \quad (16)$$

applicable just behind the scattering atom, where the complex evolution of the particle flux distribution has no distance to develop and only the momentum instant change, described by the same of the wave function phase

$$\begin{aligned} & \int_{at} \delta U(x - x_n, y - y_n, z - z_n) \frac{dz}{v} \\ = & \frac{Z\alpha}{\pi v} \int \int \left(e^{-i\chi_x x_n - i\chi_y y_n} - e^{-(\chi_x^2 + \chi_y^2 \sec^2 \psi) u_1^2 / 2 - ik_y z \tan \psi \sec \psi} \right) e^{i\chi_x x + i\chi_y y} \frac{d\chi_x d\chi_y}{\chi^2 + \kappa^2} \end{aligned} \quad (17)$$

should be considered. The found solution $\Psi(\mathbf{r}) = e^{ip_z z} f(\mathbf{r}) \varphi(x)$ will make it possible to evaluate the average increment of channeling particle transverse energy in Section III.

Before to evaluate the latter, a few points, related with the atomic string consideration, should be clarified. First, the interatomic d_{at} , inter-string d_{st} and inter-plane d distances satisfy altogether the condition $n_0 = d_{at} d_{st} d$. The planar nuclear density (4) is related with the axial one by the averaging over the distance $d_{st} / \sin \psi$, passed by a particle between the neighbouring atomic string:

$$n_n(x_n) = \int_{-\infty}^{\infty} n_n(x_n, y_n, z - z_{ax}) \frac{dz}{d_{at} / \sin \psi}. \quad (18)$$

In general, the choice of the string orientation angle ψ from Fig. 2 can considerably influence the planar channeling. Namely, at $\psi \leq \vartheta_{ch}^{ax}$, where ϑ_{ch}^{ax} is the angle of axial channeling, the latter takes place, while at $\psi \gg 1^\circ$ the irregular scattering by the high-index strings of the plane yz becomes possible [59]. To make the planar channeling certainly regular, we assume below that $\vartheta_{ch}^{ax} \ll \psi \leq 1^\circ$, assuring both the absence of the above-mentioned effects and the easily predictable picture of the incoherent scattering in the yz plane, also described by Eq. (17). Finally, the inequality $1 - \cos \psi \ll 10^{-3}$ makes it possible to put both $\sin \psi = \psi$ and $\cos \psi = 1$ below.

III. MEAN SQUARE ANGLE OF THE INCOHERENT SCATTERING OF A CLASSICALLY MOVING PARTICLE

The average transverse energy increment, induced by the incoherent particle scattering by nuclei, is applied to introduce the mean square scattering angle per a unit length of a

classically moving particle trajectory in this section. Both the solutions of Eqs. (6), (15) and the residual atomic potential property

$$\int \int \delta U(\mathbf{r} - \mathbf{r}_n) n_n(x_n, y_n, z) dx_n dy_n = 0 \quad (19)$$

allow one to represented the average incoherent transverse energy increment over a unit time, corresponding to the crystal length $\Delta z = v$, in the form

$$\begin{aligned} \langle \Delta \varepsilon_n \rangle &= \int_0^v \int_{-\infty}^{\infty} \int_{-\infty}^{\infty} \left(\int \psi^* \hat{H} \psi dx - \int \varphi^* \hat{H}_0 \varphi dx \right) n_n(x_n, y_n, z) dx_n dy_n dz \\ &= \frac{\pi v}{\xi' d_{st}} \int_{-\infty}^{\infty} \int_{-\infty}^{\infty} \int_{-\infty}^{\infty} \int_{-\infty}^{\infty} \left(\int_{-\infty}^{\infty} \frac{d}{dx} \delta U(x - x_n, y - y_n, z - z_n) \frac{dz}{v} \right)^2 n_n(\rho_n) dx_n dy_n \\ &\quad \times Ai^2(x - x_0) dx dy. \end{aligned} \quad (20)$$

The latter demonstrates that the residual potential (12) introduction is justifies by the considerable Eq. (20) simplification through the nullification of the terms, linear in both the first and the second derivatives of the former. The explicit form of both Eq. (8) and (17) reveals a pair of readily integrable Dirac functions. Along with the Gauss integration, the former allows one to reduce Eq. (20) to the form

$$\begin{aligned} \langle \Delta \varepsilon_n \rangle &= -\frac{Z^2 \alpha^2 n_0 d}{\pi v^2 \xi'^2} \int_{-\infty}^{\infty} \int_{-\infty}^{\infty} \int_{-\infty}^{\infty} \int_{\frac{|\zeta - \eta|}{2} < q_2} \frac{e^{-(\zeta + \eta)^2 u_1^2 / 2} - e^{-(\zeta^2 + \eta^2) u_1^2 / 2}}{(\zeta^2 + \chi_y^2 + \kappa^2)(\eta^2 + \chi_y^2 + \kappa^2)} \\ &\quad \times \exp \left[i x_0 (\zeta + \eta) + \frac{2i}{3} \left(\frac{\zeta + \eta}{2 \xi'} \right)^3 + i \frac{\zeta + \eta}{\xi'} t^2 \right] \zeta d\zeta \eta d\eta dt d\chi_y \end{aligned} \quad (21)$$

with the common for the Coulomb scattering integration limit, discussed in Section IV. A novel cubic term of the last Eq. (21) exponent is related with the quantum under-barrier particle penetration, being negligible under $\xi' u_1 \gg 1$, or at the particle energies

$$\varepsilon \gg \frac{1}{e E u_1^3} < 1 \text{ GeV}, \quad (22)$$

and will be further neglected.

Being an average over the particle positions, the energy increment (21) is appropriate to estimate both the averaged mean square scattering angle and dechannelling length. However, to characterize the incoherent scattering at any point of particle trajectory, one needs a local value of the mean square scattering angle per unit length. The latter can be extracted from Eq. (21) using the large momentum limit (A4) of the mean square angle of Coulomb scattering at the local nuclear density $n(x)$. To apply the latter, let us represent Eq. (21) in

the form of the integral over the particle coordinate x , readily introduced using the integral representations

$$\begin{aligned} \int_{-\infty}^{\infty} \exp \frac{2ikt^2}{\xi'} dt &= \sqrt{\xi'} \int_{x_0}^{\infty} \exp [2ik(x - x_0)] \frac{dx}{\sqrt{x - x_0}} \\ &\simeq \frac{\xi'^2}{\varepsilon} \int_{x_0}^{\infty} \exp [2ik(x - x_0)] \frac{dx}{v_x(x)}. \end{aligned} \quad (23)$$

Treating the combinations

$$q_x = \frac{\zeta - \eta}{2}, \quad q_y = \chi_y, \quad (24)$$

$$q_1 < \sqrt{x_x^2 + q_y^2} < q_2 \quad (25)$$

as the components of the transferred momentum and representing Eq. (21) in the form

$$\frac{2\varepsilon \langle \Delta \varepsilon_n \rangle}{p^2} = \int_{x_0}^{\infty} \left\langle \frac{d\theta_x^2(x)}{dz} \right\rangle \frac{v dx}{v_x(x)}, \quad (26)$$

one can introduce the local mean square projected angle of incoherent scattering per unit length

$$\begin{aligned} \left\langle \frac{d\theta_x^2(x, q_2, q_1)}{dz} \right\rangle &= \frac{4Z^2 \alpha^2 n_0 d}{\pi p^2 v^2} \int_{q_1}^{q_2} \int_0^{2\pi} \int_{-\infty}^{\infty} \frac{\exp(-2k^2 u_1^2) - \exp[-(q^2 + k^2)u_1^2]}{[(q_x + k)^2 + q_y^2 + \kappa^2][(q_x - k)^2 + q_y^2 + \kappa^2]} \\ &\quad \times (q_x^2 - k^2) \exp(2ikx) dk d\varphi q dq. \end{aligned} \quad (27)$$

Besides the integration over the transferred momentum ($q_x = q \cos \varphi$, $q_y = q \sin \varphi$), the latter contains the same over the variable $k = (\zeta + \eta)/2$, taking into consideration the interference effects in scattering by inhomogeneously distributed atoms of the crystal plane.

It is shown in Appendix B that Eq. (27) alternatively follows from the Wigner function approach [50], developed for the axial case. Both the latter and the present approach make it possible to get the similar expression for the mean square angle (B4) in the plane yz , opening up alternative methods of the developed theory experimental verification. The agreement of Eqs. (27) and (B2) demonstrates both their independence on the particle distribution and the possibility of the classical treatment of the latter at high energies.

The lower integration limit q_1 has been timely introduced just to demonstrate that both Eq. (27) and (B4) reduce to the standard Coulomb scattering theory predictions for the mean square projected scattering angle (A4) in the high transferred momentum limit of $q \gg 1/u_1$. Below we put $q_1 = 0$ and concentrate on the choice of the upper integration limit q_2 in Eq. (27).

Using the Feynman integral [60] and introducing the integration variables $q_x \pm k$, Eq. (27) is readily represented in the form

$$\begin{aligned}
\left\langle \frac{\theta_x^2(x, q_2)}{dz} \right\rangle &= \frac{4\pi Z^2 \alpha^2 n(x)}{p^2 v^2} \left[\delta \ln(x, q_2) + \ln \left(1 + \frac{q_2^2}{\kappa^2} \right)^{1/2} - \frac{q_2^2}{2(q_2^2 + \kappa^2)} \right] \\
&= \frac{2Z^2 \alpha^2 n_0 d}{p^2 v^2} \left\{ \int_{-\infty}^{\infty} \left[\frac{2k^2 - q_2^2}{2k \sqrt{q_2^2 + k^2 + \kappa^2}} \ln \left(\frac{\sqrt{q_2^2 + k^2 + \kappa^2} + k}{\sqrt{q_2^2 + k^2 + \kappa^2} - k} \right) \right. \right. \\
&\quad \left. \left. - \frac{k}{\sqrt{k^2 + \kappa^2}} \ln \left(\frac{\sqrt{k^2 + \kappa^2} + k}{\sqrt{k^2 + \kappa^2} - k} \right) \right] \exp(2ikx - 2k^2 u_1^2) dk \right. \\
&\quad \left. - \frac{2}{\pi} \int_0^{q_2} \left(\int_{-\infty}^{\infty} \frac{\sin(kx) \exp(-k^2 u_1^2/2)}{k^2 + q^2 + \kappa^2} k dk \right)^2 \exp(-q^2 u_1^2) dq \right. \\
&\quad \left. + \frac{\sqrt{\pi}}{\sqrt{2} u_1} \exp \left(-\frac{x^2}{2u_1^2} \right) \ln \left(1 + \frac{q_2^2}{\kappa^2} \right) \right\} \tag{28}
\end{aligned}$$

with the integration orders reduced from three to one and two. Eq. (28) reflects that, following the basic papers [21, 61, 63, 70], all the modifications of the incoherent scattering process by the atom distribution inhomogeneity can be grouped into the correction $\delta \ln(x, q_2)$ to the logarithm of the basic Coulomb scattering formulae from Appendix A. Fig. 3 demonstrates that $\delta \ln(x, q_2)$ gathers its value mainly at the momentum values $q \sim 1/u_1$, related by the uncertainty principle with the thermal vibration amplitude u_1 . Fig. 3 also demonstrates that $\delta \ln(x, q_2)$ becomes negative at any q_2 in the region $x < 2u_1$, describing the effect of incoherent scattering reduction there, as well as at $q_2 \leq 1/u_1$ in the region $x \gg u_1$, demonstrating the need in a special simulation approach.

IV. A CONCISE INCOHERENT SCATTERING SIMULATION METHOD

A. The multiple scattering simulation limited role

The multiple scattering angle equation (27) will now be incorporated into the simulation procedure of incoherent scattering at arbitrary momentum transfers. The former, in fact, does not provide an adequate simulation tool by itself, though can be applied for the approach [67] refinement. It should be emphasized [50], that the wide applicability of the multiple Coulomb scattering theory for macroscopic targets in no way justifies the same for channeling. The point is that the former is adequate only when the root mean square scattering angle (A2) exceeds all or most of the single scattering angles, making the particle deflection looking as a smooth continuous diffusion-like process [71, 72]. However the

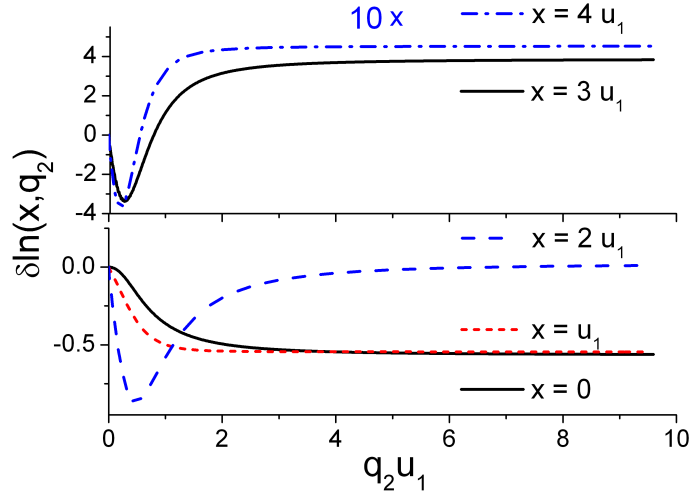


FIG. 3: Dependence of the Coulomb scattering logarithm modification on the integration limit of Eq. (28) at $x = 0, 1, 2, 3$ and $4 u_1$. The case of (110) Si planes at $T=293$ K is considered

channeling simulations rely on the thousand and million times shorter sub-micron trajectory steps within which single scattering angles mostly far exceed that of the multiple scattering, making the trajectory steps looking like an angle. This, effectively, "large" angle single scattering, in particular, is responsible for the stochastic nature of both the particle trajectories and transverse energy evolution, including both sudden dechanneling and rechanneling occasions. None of the latter can be described by the established multiple scattering theory, making impossible to introduce the upper limit to Eqs. (A2)-(A4) consistently [11]. That is why the multiple scattering simulations must be reduced to the minimum, determined by the quantum effects [50].

B. The enhanced power of the Coulomb scattering logarithm modification

No problems of the cross section definition surely appear in the multiple Coulomb theory in the uniform medium. However, the situation changes in the presence of a plane or a string atom inhomogeneity. Namely, the cross section, formally extracted from Eqs. (B2)-(B4) following a requirement of its approaching the Coulomb value (A1) at $q \gg 1/u_1$, proves to be negative at $q \leq 1/u_1$ [50]. This uncommon circumstance makes the routine simulations impossible and should be considered as a natural consequence of the transversely

”nonlocal” quantum scattering process reduction to the classical trajectory. However, since the extracted cross section attains negative values at the small momenta $q \leq 1/u_1$ only, they can be readily ”absorbed” by the mean square angle integrals, which can be readily made positive by the integration limit q_2 extension.

The latter, at the same time, secures a positive meaning of the extracted modified cross section [50], making it valid for the single scattering sampling at $q > q_2$. However, since the latter requires additional operations, more effective will be to sample the unperturbed Coulomb scattering, including the large momentum scattering modification effect into the mean square multiple scattering angle. To introduce the latter, the multiple Coulomb scattering theory prediction (A3) for a uniform medium with nuclear density $n(x)$ has been separated out in Eq. (28).

As Fig. 3 demonstrates, the logarithm modification value $\delta \ln(x, q_2)$, introduced in Eq. (28) to put together all the effects of the atom distribution inhomogeneity, converges fast to the limit

$$\begin{aligned} \delta \ln(x) = \delta \ln(x, q_2 \gg 1/u_1) &= \frac{u_1^2 - x^2}{3u_1^4(q_2^2 + \kappa^2)} \\ &- \left\{ \int_{-\infty}^{\infty} \frac{k}{\sqrt{k^2 + \kappa^2}} \ln \left(\frac{\sqrt{k^2 + \kappa^2} + k}{\sqrt{k^2 + \kappa^2} - k} \right) \exp(2ikx - 2k^2u_1^2) dk \right. \\ &+ \left. \frac{2}{\pi} \int_0^{\infty} \left(\int_{-\infty}^{\infty} \frac{\sin(kx)}{(k^2 + q^2 + \kappa^2)} \exp\left(\frac{-k^2u_1^2}{2}\right) k dk \right)^2 \exp(-q^2u_1^2) dq \right\} \frac{u_1}{\sqrt{2\pi}} \exp\left(\frac{x^2}{2u_1^2}\right), \end{aligned} \quad (29)$$

reducing Eq. (28) to

$$\left\langle \frac{\theta_x^2(x, q_2)}{dz} \right\rangle = \frac{4\pi Z^2 \alpha^2 n(x)}{p^2 v^2} \left[\delta \ln(x) + \ln \left(1 + \frac{q_2^2}{\kappa^2} \right)^{1/2} - \frac{q_2^2}{2(q_2^2 + \kappa^2)} \right]. \quad (30)$$

The first term of Eq. (29) is, strictly speaking, negligible at $q_2 = \vartheta_{max}/p$, where ϑ_{max} is the maximal nuclear scattering angle of the logarithmic approximation, and is shown only to recognize that the preservation of the κ^2 term in the sum $q_2^2 + \kappa^2$ exceeds the real precision, serving only the purpose of the Eq. (30) correspondence to the canonical equation (A3). Eq. (30) makes it possible to locally describe the incoherent scattering, on the one hand, of the electrons, moving in the dense nuclear regions, and, on the other, of both protons and positrons, stably channeling in the negligible density ones. The average value of the same can be applied to the case of the uniform particle flux distribution realized at large incidence angles, described by the Eq. (30) average

$$\overline{\delta \ln(x)} \equiv \frac{1}{d} \int_0^d \delta \ln(x) dx = - \int_0^{\infty} \frac{q^2 \exp(-q^2u_1^2)}{2(q^2 + \kappa^2)^2} dq^2 \simeq -0.43, \quad (31)$$

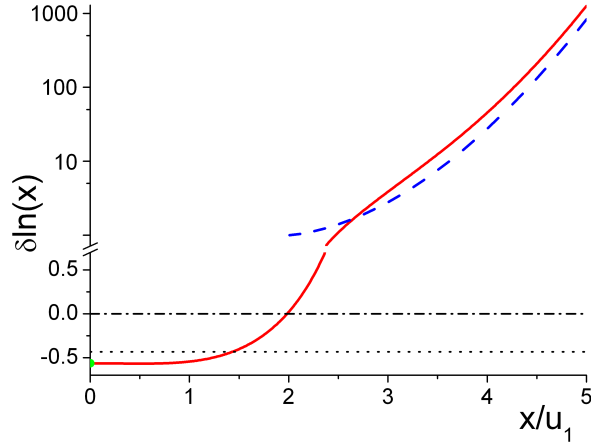


FIG. 4: The x -coordinate dependence of the logarithm modification (29), describing the incoherent scattering difference from that in amorphous medium of the same density. Dashed line depicts the asymptote (C5), while dotted one the average value of the same effect (31) in the high incidence angle limit [57]. The case of (110) Si planes at T293 K is considered.

quantifying the effect of incoherent scattering reduction in crystals, predicted in [57] and measured in [59].

C. The local scattering approximation and its violation at $x \gg u_1$

Fig. 4 illustrates the coordinate dependence of both the logarithm modification (29) and its leading expansion term evaluated in Appendix C, evaluated for the (110) Si plane at $u_1 = 0.075 \text{ \AA}$, which demonstrates qualitatively different behavior in the regions of high, $x < u_1$, and low, $x > 2u_1$, nuclear density. Indeed, at $x \leq u_1$ the Gaussian integrals in Eq. (30) form at small $k \sim 1/u_1$, making it possible to treat (A5) independently from the integration over q starting from a rather low Eq. (A4) limit $q_1 \simeq 1/u_1$, revealing the proportionality to the local nuclear density $n(x)$. The only noticeable modification of the (27) integral occurs at $q \leq q_1 \simeq 1/u_1$, which, given the κ^2 presence in the denominator, results in the logarithm reduction of $\delta \ln(x \leq u_1) \simeq -0.57$. The latter locally describes the effect of incoherent scattering reduction, being both closely related to the experimentally observed [59] average effect (31) and directly applicable to the electron channeling.

Being both natural and indirectly confirmed by the experiment at $x \leq u_1$, the local

scattering approximation causes reasonable doubts at $x \gg u_1$. Indeed, first, the rapid increase of the Coulomb denominator at $k \geq \kappa$ disturbs the Gaussian integral formation, which occurs at the larger $k \sim x/u_1^2 \gg 1/u_1$. Second, the averaged atomic field decreases like the exponential function $e^{-\kappa x}$, or much slower than the Gaussian (4). By this reason the thermal atom field fluctuations must both give the dominant contribution to the local mean square incoherent scattering angle at $x \gg u_1$ and be proportional to the product $u_1^2 e^{-2\kappa x}$. This mechanism, called [73] the one-phonon excitation, was suggested by J. Lindhard [1] and verified experimentally [49, 74, 75] in the axial case in 80-th. Fig. 4 illustrates the similar predictions, obtained in the planar case by the direct numerical evaluation and confirmed by the analytical estimate in Appendix C.

The revealed incoherent scattering mechanism in no way can be coordinated with the local approximation in which the local nuclear density is directly substituted into Eq. (A2). Indeed, since the formula (A2) embraces all the possible scattering angles, its solitary use assumes the full neglect of the large angle catastrophic scattering processes as well as unnatural reduction of all the stochastic features of particle motion. At the same time, despite the drastic Coulomb logarithm overestimation, the vanishing nuclear density factor results, in total, in the underestimation of the mean square incoherent scattering angle at $x > 3u_1$.

D. The incoherent scattering sampling

Eqs. (29), (30) make it possible to describe the incoherent scattering in the regions of both the high and negligible nuclear density. However, according to the opposite logarithm (29) signs (see Fig. 4), the simulation algorithms considerably differ at $x \leq u_1$ and $x \gg u_1$. Indeed, if $\delta \ln(x) < 0$, the incoherent scattering process can be sampled in full as a Coulomb scattering by the angles $q > q_2^0/p$, limited from below by the momentum transfer q_2^0 , determined by the equation

$$\left\langle \frac{d\theta_x^2(x, q_2^0)}{dz} \right\rangle = 0. \quad (32)$$

At this, all the incoherent scattering modifications are taken into consideration by abandoning of the momentum transfers of $q < q_2^0$.

At $\delta \ln(x) > 0$, on the opposite, the Coulomb scattering is sampled for any $q > 0$, however, to take into consideration the scattering on individual phonons, described by the large positive logarithm modification (29) from Fig. 4, a random scattering, characterized

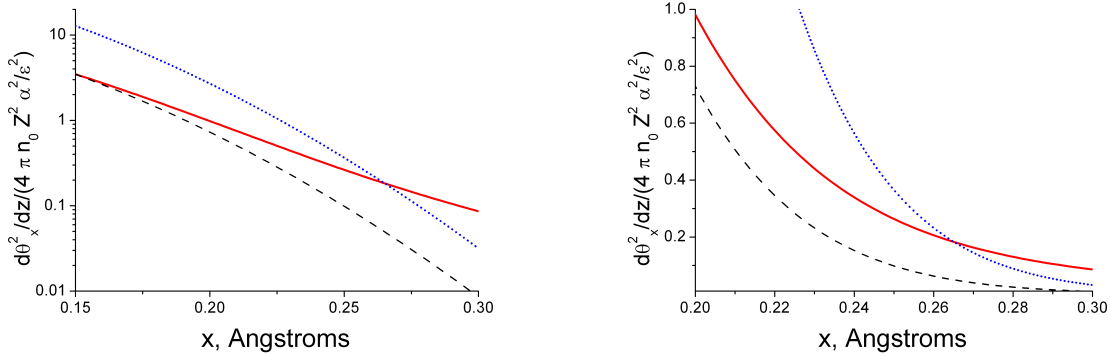


FIG. 5: The x -coordinate dependence of the local mean square projected scattering angles per unit length: solid red line – determined by Eq. (30), dashed black – by the same with $\delta \ln(x) = 0$ and dotted blue – by Eq. (A2)). All the values are normalized to $4\pi Z^2 n_0 \alpha^2 / \varepsilon^2$. The same data are depicted on the left and on the right, in logarithmic and linear scales, respectively

by the mean square angle

$$\left\langle \frac{d\theta_x^2(x, q_2)}{dz} \right\rangle = \frac{4Z^2 \alpha^2 n(x)}{p^2 v^2} \delta \ln(x), \quad (33)$$

should be additionally sampled. Fig. 4 demonstrates that the latter can reach drastic relative values, reflecting the distant one-phonon excitation predominance over the local scattering.

To compare the roles of different scattering mechanisms, the corresponding mean square angles are compared in Fig. 5 in the case of (110) Si planes and positron energy of 1.5 GeV, corresponding to the "optimal" crystal undulator construction, suggested in [30]. To reveal the role of the Coulomb scattering at local density, the solid curve, evaluated using Eq. (30), is compared with the dashed one, evaluated using the same with $\delta \ln(x)$ put to zero. While the latter curve approaches the former one at the considerably nuclear densities, at $x \sim 2u_1$ it becomes inferior, when the scattering on individual phonons dominates. Comparing further the solid curve with the dotted one, built according to Eq. (A2) to represent the predictions of the local scattering approximation [67, 69], one concludes that the latter both overestimates the scattering intensity at the high, and underestimates it at the low nuclear densities. The difference in prediction of Eqs. (30) and (A2) would be even deeper if the overestimated Coulomb logarithm of the latter has not been compensated by the multiplication by the vanishing nuclear density. Note that the particular value of q_2 in Eq. (30), which was fixed by the condition $q_2^2/2\varepsilon = U(2u_1)$, has a marginal effect on the

revealed predictions.

It should be clarified, that the described sampling receipts do not precisely reflect the real physical peculiarities of the scattering process, representing only the technical means to incorporate the thoroughly evaluated mean square incoherent scattering angles into the classical trajectory simulations.

In general, the overestimated growth of incoherent scattering intensity (the dotted blue curve in Fig. 5) supports the assumption [11] of the instant "turning on" of the nuclear scattering at some distance $x \sim 1/\kappa$ from the plane. Being adopted, in fact, from the nonrelativistic ion channeling theory, this approach loses its applicability at multi-Gev energies. The demonstrated above slowdown of the decrease of incoherent scattering intensity with transverse coordinate (see the solid red curve in Fig. 5), on the opposite, strengthens the picture of the nuclear dechanneling process widely distributed both in longitudinal and transverse directions [55], being poorly treated by the single dechanneling length approach.

E. The lack of a consistent electron scattering theory

The process of incoherent particle scattering by the electrons of medium atoms, called shortly the electron scattering, gives a roughly Z -times smaller contribution to the mean square Coulomb scattering angle than the nuclear one, being often treated approximately [61, 70]. However, the electron scattering can take over the leading role in the low nuclear density regions of the stable positively charged particle channeling, making necessary its quantitative consideration in crystals.

Contrary to the multiple scattering, particle collisions with electrons are essential for the ionization energy loss process, the theory of which is well developed accordingly [60, 65, 66, 70, 71]. The latter reveals that relativistic particles efficiently transfer their energy to electrons at impact parameters far exceeding the inter-atomic distance in condensed medium, making the local consideration of the ionization losses in crystals even less appropriate, than for the nuclear scattering.

Though the treatment of the ionization energy losses in the inhomogeneous electron distribution of atomic strings and planes is already known [76–78], its application to the process of electron multiple scattering is not straightforward by the reason that particle deflection is related solely with the transverse momentum transfer, while the ionization losses are with

both transverse and longitudinal ones. Giving no contribution to the multiple scattering, the latter dominates at relativistic ionization energies. However, since the transverse channeling motion becomes relativistic [2–6] at the particle energy of $m^2/2V_0 \sim 0.1 - 10$ GeV, the latter case becomes quite common in the TeV-energy region, making the seminal ionization loss formula [80] inapplicable for the mean square scattering angle evaluation and revealing thus the need in its alternative.

Longitudinal momentum component also dominates near the threshold of the atom excitation or ionization, which determines the minimal value of the former, being essential for both the Coulomb logarithm and density effect reconsideration. Finally, the electron multiple scattering theory should be enriched by the temperature depending Debye-Waller factor, both the partial and full atomic form factors [81, 82] as well as the incoherent scattering function [63, 83].

V. CONCLUSIONS

The theory, which describes the incoherent particle scattering by atomic planes with neither arbitrary assumptions nor phenomenological parameter introduction has been developed. The obtained formula for the mean square scattering angle of incoherent scattering proves to be in agreement with the alternative approach [50], developed for the axial case. Both of them predict the modest incoherent scattering suppression in the dense nuclear regions as well as the inapplicability of the local scattering treatment far from the latter. All the quantum features of incoherent scattering are accumulated in the Coulomb logarithm modification (29). The latter secures the minor amendments of the Coulomb scattering sampling, which take into consideration the influence of the crystal plane atom distribution heterogeneity on the incoherent scattering of relativistic particles moving along classical trajectories. Though the present theory has been developed for the case of channeling motion, we envisage its wider application, demonstrated by the agreement both with the uniform particle flux limit (31) [57, 59] and the axial case [50]. Similarly to latter, the developed approach makes it possible to refine the numerical treatment of any experiment on high energy particle scattering and radiation in the fields of crystal planes ever conducted or planned.

Financial support by the European Commission through the N-Light Project, Grant Agreement number: 872196, is gratefully acknowledged.

VI. APPENDIX A

The developed incoherent scattering consideration should be integrated into the established Coulomb scattering theory. The most acknowledged [68] version of the latter proceeds from the simple screened Coulomb cross section

$$\frac{d^2\sigma_C(q)}{dq^2} = \frac{4Z^2\alpha^2}{v^2(q^2 + \kappa^2)^2}, \quad (A1)$$

leading to the widely used formula

$$\frac{d\theta_{space}^2}{dz} = 2\frac{d\theta_0^2}{dz} = n \int_0^{\vartheta_{max}p} \frac{q^2}{p^2} \frac{d^2\sigma_C(q)}{dq^2} dq^2 = \left(\frac{21MeV}{vp}\right)^2 L_{rad}^{-1} \simeq \frac{8\pi Z^2\alpha^2 n}{p^2 v^2} \ln \frac{\vartheta_{max}}{\vartheta_{min}} \quad (A2)$$

for both the mean square nonprojected (space) d^2_{space}/dz and projected (plane) $d\theta_0^2/dz$ scattering angles (we use both the notations and terminology of [80]) in amorphous media with atomic number Z and nuclear density n , $\vartheta_{min} = \kappa/p$ and ϑ_{max} are respectively the typical atom and maximal nuclear scattering angles. Since the atomic plane consideration assumes the azimuthal symmetry violation, we consider mainly the mean square projected (plane) angles in both the channeling xz (27), (28), (30), (B3) and the normal to it yz (B4) planes, both of which should be compared with the same in amorphous media $d\theta_0^2/dz$, being, according to Eq. (A2), twice as less as the nonprojected (space) one. In particular, we will use the mean square projected scattering angle for both the limited, $0 < q < q_2$,

$$\frac{d\theta_0^2(q < q_2)}{dz} = \frac{1}{2}n \int_0^{q_2} \frac{q^2}{p^2} \frac{d^2\sigma_C(q)}{dq^2} dq^2 = \frac{4\pi Z^2\alpha^2 n}{v^2 p^2} \left[\ln \left(1 + \frac{q_2^2}{\kappa^2}\right)^{1/2} - \frac{q_2^2}{2(q_2^2 + \kappa^2)} \right] \quad (A3)$$

and asymptotic, $q_1 \gg \kappa$, $q_2 \gg q_1$,

$$\frac{d\theta_0^2(q_1 < q < q_2)}{dz} = \frac{1}{2}n \int_{q_1}^{q_2} \frac{q^2}{p^2} \frac{d^2\sigma_C(q)}{dq^2} dq^2 \simeq \frac{4\pi Z^2\alpha^2 n}{v^2 p^2} \ln \frac{q_2}{q_1} \quad (A4)$$

momentum transfers, the latter of which corresponds to the high momentum transfer limit

$$\left\langle \frac{d\theta_x^2(x)}{dz} \right\rangle \simeq \frac{4Z^2\alpha^2 n_0 d}{\pi p^2 v^2} \int_{q_1}^{q_2} \int_0^{2\pi} \int_{-\infty}^{\infty} \frac{q_x^2 \exp(2ikx - 2k^2 u_1^2)}{(q^2 + \kappa^2)^2} dk d\varphi q dq \quad (A5)$$

of Eq. (27) at local nuclear density $n = n_n(x)$, given by Eq. (4), as is readily seen from the integral

$$\int_{-\infty}^{\infty} \exp(2ikx - 2k^2 u_1^2) dk = \frac{\sqrt{\pi}}{\sqrt{2} u_1} \exp\left(-\frac{x^2}{2u_1^2}\right) = \frac{\pi n_n(x)}{n_0 d} \quad (A6)$$

and will be used to extract the effective local mean square projected angle per unit length (27) for arbitrary momentum transfers.

VII. APPENDIX B

The central result (27) is reproduced below using the Wigner function

$$\begin{aligned}
W_{\rho_n}(\boldsymbol{\rho}, \mathbf{q}) &= -\frac{8Z\alpha}{\pi v} \left[\frac{\cos 2\mathbf{q}(\boldsymbol{\rho} - \boldsymbol{\rho}_n) - \cos(2\mathbf{q}\boldsymbol{\rho}) \exp(-2q^2 u_1^2)}{4q^2 + \kappa^2} \right] \\
&+ \frac{4Z^2\alpha^2}{\pi^2 v^2} \int \exp(2i\mathbf{k}\boldsymbol{\rho}) \left\{ \frac{\exp[-i(\mathbf{q} + \mathbf{k})\boldsymbol{\rho}_n] - \exp[-(\mathbf{q} + \mathbf{k})^2 u_1^2/2]}{(\mathbf{q} + \mathbf{k})^2 + \kappa^2} \right\} \\
&\quad \times \left\{ \frac{\exp[i(\mathbf{q} - \mathbf{k})\boldsymbol{\rho}_n] - \exp[-(\mathbf{q} - \mathbf{k})^2 u_1^2/2]}{(\mathbf{q} - \mathbf{k})^2 + \kappa^2} \right\} d^2k \\
&- \frac{4Z^2\alpha^2}{\pi^2 v^2} \exp(2i\mathbf{q}\boldsymbol{\rho}) \int \left\{ \frac{\exp[-i(\mathbf{q} + \mathbf{k})\boldsymbol{\rho}_n] - \exp[-(\mathbf{q} + \mathbf{k})^2 u_1^2/2]}{(\mathbf{q} + \mathbf{k})^2 + \kappa^2} \right\} \\
&\quad \times \left\{ \frac{\exp[-i(\mathbf{q} - \mathbf{k})\boldsymbol{\rho}_n] - \exp[-(\mathbf{q} - \mathbf{k})^2 u_1^2/2]}{(\mathbf{q} - \mathbf{k})^2 + \kappa^2} \right\} d^2k,
\end{aligned} \tag{B1}$$

obtained by an alternative method in the axial case [50]. The mean square angles of incoherent scattering in the planes xz and yz

$$\begin{aligned}
\left\langle \frac{\theta_i^2(\boldsymbol{\rho})}{dz} \right\rangle &= \int \int \int \int \frac{q_i^2}{p^2} W_{\rho_n}(\boldsymbol{\rho}, \mathbf{q}) n_n(\rho_n, 0) d^2q d^2\rho_n = \frac{4Z^2\alpha^2}{\pi^2 v^2 p^2 d_{at}} \\
&\times \int \int \int \int \frac{\exp[-2k^2 u_1^2] - \exp[-(k^2 + q^2)u_1^2]}{[(\mathbf{q} + \mathbf{k})^2 + \kappa^2][(\mathbf{q} - \mathbf{k})^2 + \kappa^2]} (q_i^2 - k_i^2) \exp(2i\mathbf{k}\boldsymbol{\rho}) d^2k d^2q
\end{aligned} \tag{B2}$$

are obtained by Eq. (B1) multiplication by q_i^2 , $i = x, y$, integration over \mathbf{q} and averaging over the string atom nuclei distribution, following from Eq. (14) at $\psi = 0$. Both the integrand symmetry and variable notation interchange of $\mathbf{q} \leftrightarrow \mathbf{k}$ have been used in the above transformation as well. To reduce Eq. (B2) to the planar case, it is integrated further over $y = \psi z$, resulting in the Dirac delta function $\delta(2k_y)$, absorbed by the integration over k_y , yielding both the mean square scattering projected (plane) angle per unit length in both the xz

$$\begin{aligned}
\left\langle \frac{\theta_x^2(x)}{dz} \right\rangle &= \int \left\langle \frac{\theta_x^2(\boldsymbol{\rho})}{dz} \right\rangle \frac{dy}{d_{st}} = \frac{4Z^2\alpha^2 n_0 d}{\pi p^2 v^2} \\
&\times \int \int \int \frac{\exp(-2k^2 u_1^2) - \exp[-(k^2 + q^2)u_1^2]}{[(q_x + k)^2 + q_y^2 + \kappa^2][(q_x - k)^2 + q_y^2 + \kappa^2]} (q_x^2 - k^2) \exp(2ikx) dk d^2q
\end{aligned} \tag{B3 \equiv 27}$$

and yz plane

$$\begin{aligned}
\left\langle \frac{\theta_y^2(x)}{dz} \right\rangle &= \int \left\langle \frac{\theta_y^2(\boldsymbol{\rho})}{dz} \right\rangle \frac{dy}{d_{st}} = \frac{4Z^2\alpha^2 n_0 d}{\pi p^2 v^2} \\
&\times \int \int \int \frac{\exp(-2k^2 u_1^2) - \exp[-(k^2 + q^2)u_1^2]}{[(q_x + k)^2 + q_y^2 + \kappa^2][(q_x - k)^2 + q_y^2 + \kappa^2]} q_y^2 \exp(2ikx) dk d^2q,
\end{aligned} \tag{B4}$$

the latter of which can alternatively be obtained using $\hat{H}_0\varphi = \hat{p}_y^2/2\varepsilon$ instead of Eq. (3).

VIII. APPENDIX C

To demonstrate the asymptotic behavior of Eq. (27) at large x , let us represent its first integral in the form

$$\int_{-\infty}^{\infty} \int_{-\infty}^{\infty} \int_{-\infty}^{\infty} \frac{\exp[-(q_x^2 + k^2)u_1^2 + 2ikx] \times (q_x^2 - k^2)}{[(q_x + k)^2 + q_y^2 + \kappa^2][(q_x - k)^2 + q_y^2 + \kappa^2]} \sum_{n=0}^{\infty} \frac{1}{n!} [(q_x - k)^2 u_1^2]^n dk dq_x dq_y. \quad (C1)$$

All the integrals both over k and q_x are connected with the one

$$\begin{aligned} \int_{-\infty}^{\infty} \frac{\exp(-k^2 u_1^2/2 + ikx)}{k^2 + q_y^2 + \kappa^2} dk &= \exp[(q_y^2 + \kappa^2)u_1^2/2] \left(\int_{-\infty}^{\infty} \frac{\exp[-\alpha(k^2 + q_y^2 + \kappa^2)u_1^2/2 + ikx]}{k^2 + q_y^2 + \kappa^2} dk \right)_{\alpha=1} \\ &= \frac{\pi}{\sqrt{q_y^2 + \kappa^2}} \exp[(q_y^2 + \kappa^2)u_1^2/2 - \sqrt{q_y^2 + \kappa^2} x] \\ &\quad - \sqrt{2\pi} u_1 \exp[(q_y^2 + \kappa^2)u_1^2/2] \int_0^1 \exp\left[-\frac{1}{2}\beta^2(q_y^2 + \kappa^2)u_1^2 - \frac{x^2}{2\beta^2 u_1^2}\right] d\beta \\ &\simeq \frac{\pi}{\sqrt{q_y^2 + \kappa^2}} \exp[(q_y^2 + \kappa^2)u_1^2/2 - \sqrt{q_y^2 + \kappa^2} x]. \end{aligned} \quad (C2)$$

In order to separate the local contribution of the nuclear density above, a first order differential equation has been introduced by means of taking a derivative over the fictitious parameter α . Eq. (C2) can be readily applied to approximate the integral

$$\begin{aligned} \int_{-\infty}^{\infty} \frac{\sin(kx) \exp(-k^2 u_1^2/2)}{k^2 + q_y^2 + \kappa^2} k dk &= \pi \exp[(q_y^2 + \kappa^2)u_1^2/2 - \sqrt{q_y^2 + \kappa^2} x] \\ &\quad - \sqrt{2\pi} \frac{x}{u_1} \exp[(q_y^2 + \kappa^2)u_1^2/2] \int_0^1 \exp\left[-\frac{1}{2}\beta^2(q_y^2 + \kappa^2)u_1^2 - \frac{x^2}{2\beta^2 u_1^2}\right] \frac{d\beta}{\beta^2} \\ &\simeq \pi \exp[(q_y^2 + \kappa^2)u_1^2/2 - \sqrt{q_y^2 + \kappa^2} x], \end{aligned} \quad (C3)$$

corresponding both to the $n = 0$ term of the expansion (C1) and the second integral of Eq. (27), as well as the one of

$$\begin{aligned} \int_{-\infty}^{\infty} \frac{k^2 \cos(kx) \exp(-k^2 u_1^2/2)}{k^2 + q_y^2 + \kappa^2} dk &= \frac{\sqrt{2\pi}}{u_1} \exp\left(-\frac{x^2}{2u_1^2}\right) \\ &\quad - (q_y^2 + \kappa^2) \int_{-\infty}^{\infty} \frac{\cos(kx) \exp(-k^2 u_1^2/2)}{k^2 + q_y^2 + \kappa^2} dk \\ &\simeq -\pi \sqrt{q_y^2 + \kappa^2} \exp[(q_y^2 + \kappa^2)u_1^2/2 - \sqrt{q_y^2 + \kappa^2} x], \end{aligned} \quad (C4)$$

which represents itself the $n = 1$ term of the expansion (C1). The above integrals demonstrate that the Gaussian local nuclear density contributions to Eq. (27) are negligible at

$x \gg u_1$. Reducing them further to the MacDonald functions K_0 , K_1 , one arrives to the leading term of the Eq. (27) expansion in series in small parameter $u_1\kappa$

$$\left\langle \frac{d\theta_x^2(x, q_2, q_1)}{dz} \right\rangle \simeq \frac{4\pi Z^2 \alpha^2 n_0 d}{p^2 v^2} \kappa (u_1 \kappa)^2 \left[K_1(2\kappa x) + \frac{1}{\kappa x} K_0(2\kappa x) + \frac{1}{\kappa^2 x^2} K_1(2\kappa x) \right]. \quad (C5)$$

Note that the leading contributions to both the first and the second integrals of Eq. (27) greatly exceed (C5), however cancel each other. Since MacDonald functions exponentially decrease as

$$K_0(2\kappa x), K_1(2\kappa x) \sim \frac{1}{2} \sqrt{\frac{\pi}{\kappa x}} \exp(-2\kappa x) \quad (C6)$$

at $x > 1/\kappa$, Eq. (C5) visualizes the expected non-gaussian nonlocal behavior of the mean square scattering angle (27) at large distances from the atomic plane, corresponding both to the explosive logarithm growth, depicted in Fig. 4, and the decelerated local mean square angle decrease, illustrated in Fig. 5. As in the axial case [1], the factor $(\kappa u_1)^2$ appears in Eq. (C5) after the averaging of the square of the averaged atom field $2\pi Z \alpha \exp(-\kappa x)$ thermal perturbation.

Though the higher $n = 2, 3, \dots$ terms of the asymptotic expansion (C1) can be readily evaluated, the one-dimensional integral representation of the first three-dimensional integral of Eq. (27) proves to be more practical. In addition, the removal (C3) of the oscillating integrand simplifies the evaluation of Eqs. (27)-(29).

-
- [1] J. Lindhard, Influence of crystal lattice on motion of energetic charged particles, Phys. Lett. **12**, 126 (1964); Kgl. Dan. Vidensk. Selsk. Mat. Fys. Medd. **34** (1965) 1.
 - [2] V.G. Baryshevsky, High-Energy Nuclear Optics of Polarized Particles. World Press, 2012. 640 p. <https://doi.org/10.1142/7947>.
 - [3] V.G. Baryshevskii, V.V. Tikhomirov, Synchrotron-type radiation processes in crystals and polarization phenomena accompanying them, Usp. Fiz. Nauk **159** (1989) 529; [Sov. Phys. Usp. **32** (1989) 1013].
 - [4] A.I. Akhiezer, N.F. Shul'ga, High Energy Electrodynamics in Matter. Gordon and Breach, New York, 1996.
 - [5] V.N. Baier, V.M. Katkov, and V.M. Strakhovenko, Electromagnetic Processes at High Energies in Oriented Single Crystals (World Scientific, Singapore, 1998).

- [6] J.C. Kimball, N. Cue, Quantum electrodynamics and channeling in crystals, *Phys. Reports*, **125** (1985) 69.
- [7] E.N. Tsyganov, Some aspects of the mechanism of a charged particle penetration through a monocrystal, Fermilab TM-682 (1976).
- [8] A.M. Taratin and S.A. Vorobiev, "Volume reflection" of high-energy particles in quasi-channeling states in bent crystals, *Phys. Lett. A* **119**(1987)425.
- [9] V.V. Tikhomirov, A technique to improve crystal channeling efficiency of charged particles, *J. of Instrumentation*, **2**(2007) P08006.
- [10] V.V. Tikhomirov, Multiple volume reflection from different planes inside one bent crystal, *Phys. Lett. B*. **655** (2007) 217.
- [11] V.M. Biryukov, Yu.A. Chesnokov, and V.I. Kotov, *Crystal channeling and its application at high-energy accelerators*. (Springer, Berlin, Germany, 1997).
- [12] W. Scandale, Use of crystals for beam deflection in particle accelerators, *Mod. Phys. Lett. A*. **27** (2012) 1230007.
- [13] V.V. Tikhomirov, V.V. Haurylavets, A.S. Lobko, and V.A. Mechinsky, *Oriented Crystal Applications in High Energy Physics. Engineering of Scintillation Materials and Radiation Technologies (Proceedings of ISMART 2016)*. Springer Proceedings in Physics Volume 200. PP. 259-280.
- [14] V.A. Andreev et al., Spatial focusing of 1 GeV protons by a curved single crystal, *Pis'ma Zh. Eksp. Teor. Fiz.*, **41** (1985) 408 [*JETP Lett.* **41** (1985) 500].
- [15] W. Scandale et al., Observation of focusing of 400 GeV proton beam with the help of bent crystals, *Phys. Lett. B* **733** (2014) 366.
- [16] V.V. Tikhomirov, Can electron beams be really focused by bent crystals? arXiv: 1809.06164 [physics.acc-ph] 17 Sep 2018.
- [17] K. Elsener, G. Fidecaro, M. Gyr, W. Herr, J. Klem, U. Mikkelsen, S.P. Moller, E. Uggerhoj, G. Vuagnin, E. Weisse, Proton extraction from the CERN SPS using bent silicon crystals. *Nucl. Instrum. Meth. B* **119** (1996) 115.
- [18] J.P. Lansberg et al., A Fixed-Target Experiment at the LHC (AFTER@LHC) : luminosities, target polarisation and a selection of physics studies, arXiv:1207.3507 [hep-ex].
- [19] A. Mazzolari, E. Bagli, L. Bandiera, V. Guidi, H. Backe, W. Lauth, V. Tikhomirov, A. Berra, D. Lietti, M. Prest, E. Vallazza, and D. De Salvador, Steering of a sub-GeV electron beam

- through planar channeling enhanced by rechanneling, *Phys. Rev. Lett.* **112** (2014) 135503
- [20] A. I. Sytov, L. Bandiera, D. De Salvador, A. Mazzolari, E. Bagli, A. Berra, S. Carturan, C. Durighello, G. Germogli, V. Guidi, P. Klag, W. Lauth, G. Maggioni, M. Prest, M. Romagnoni, V. V. Tikhomirov, E. Vallazza, Steering of Sub-GeV electrons by ultrashort Si and Ge bent crystals, *Eur. Phys. J. C* **77** (2017) 901.
- [21] M.L. Ter-Mikaelian, *High-energy Electromagnetic Processes in Condensed Media* Wiley. New York, 1972.
- [22] V.N. Baier, V.M. Katkov, V.M. Strakhovenko, Hard photon emission from high energy electrons and positrons in single crystals, *Nucl. Instrum. Meth. B* **69** (1992) 258.
- [23] V.V. Tikhomirov, Possibility of observing radiative self-polarization and the production of polarized e+e- pairs in crystal at accessible energies, *JETP Lett.* **58** (1993) 166.
- [24] M.A. Kumakhov, On the theory of electromagnetic radiation of charged particles in a crystal, *Phys. Lett. A*, **57**(1976)17.
- [25] V.G. Baryshevsky, I.D. Feranchuk, and A.P. Ulyanenkov, *Parametric X-ray Radiation in Crystals*. Springer Tracts in Modern Physics. Vol. 213. 2006. 63 figs., IX, 172 pages.
- [26] V.G. Baryshevsky, A.O. Grubich, I.Ya. Dubovskaya, Generation of gamma-quanta by channeled particles in the presence of a variable external field, *Phys. Lett. A* **77** (1980) 61.
- [27] V.V. Kaplin, S.V. Plotnikov, S.A. Vorobiev, Radiation by charged particles channeled in deformed crystals, *Zh. Tekh. Fiz.* **50**(1980)1079.
- [28] A.V. Korol, A.V. Solov'yov, W. Greiner, *Channeling and Radiation in Periodically Bent Crystals*, Springer Series on Atomic, Optical, and Plasma Physics 69, Springer-Verlag Berlin Heidelberg 2013. DOI: 10.1007/978-3-642-31895-5_6.
- [29] V.G. Baryshevsky, V.V. Tikhomirov, Crystal Undulators: from the Prediction to the Mature Simulations, *Nucl. Instrum. And Methods. B* **309** (2013) 30.
- [30] V.V. Tikhomirov, A benchmark construction of positron crystal undulator. arXiv:1502.06588v1 [physics.acc-ph] 23 Feb 2015.
- [31] E. Bagli, L. Bandiera, V. Bellucci, E. Berra, R. Camattari, D.De Salvador, G. Germogli, V. Guidi, L. Lanzoni, D. Lietti, A.Mazzolari, M. Prest, V. V. Tikhomirov, and E. Vallazza, Experimental evidence of planar channeling in a periodically bent crystal. 1410.0251v1 [physics.acc-ph] 1 Oct 2014. *Eur. Phys. J. C* (2014)(10) 74:3114. DOI: 10.1140/epjc/s10052-014-3114-x
- [32] R. Camattari, L. Bandiera, V. Tikhomirov, M. Romagnoni, E. Bagli, G.Germogli, A. Sytov,

- T. Maiolino, M. Tamisari, A. Mazzolari, V. Guidi, and G. Cavoto, Silicon crystalline undulator prototypes: Manufacturing and x-ray characterization, *Phys. Rev. Accel. Beams* **22**, 044701 (2019) <https://doi.org/10.1103/PhysRevAccelBeams.22.044701>.
- [33] V.G. Baryshevsky, V.V. Tikhomirov, Birefringence of the high-energy gamma-quanta in monocrystals, *Physics of Particles and Nuclei*, **36** (1982) 408.
- [34] V. G. Baryshevsky, A.O. Grubich, Possibility of measuring the dependence of the anomalous magnetic moment of ultrarelativistic e^- (e^+) on the particle energy and external field strength, *Sov. J. Nucl. Phys.* **44** (1986) 721.
- [35] V.V. Tikhomirov, To the possibility to observe positron magnetic moment variation under the propagation through crystals, *Sov. Yad. Phys.* **57** (1994) 2302.
- [36] U. I. Uggerhoj, The interaction of relativistic particles with strong crystalline fields, *Rev. Mod. Phys.* **77** (2005) 1131.
- [37] V.G. Baryshevsky, Spin rotation of ultrarelativistic particles passing through a crystal, *Pis'ma. Zh. Tekh. Fiz.* **5** (1979) 182.
- [38] V.G. Baryshevsky, A.O. Grubich, Radiative self-polarization of fast particles in bent crystals, *Pis'ma. Zh. Tekh. Fiz.* **5** (1979) 1527.
- [39] V.G. Baryshevsky, A. O. Grubich, Self-polarization and spin precession of channeled particles, *Sov. J. Nucl. Phys.* **37** (1983) 648.
- [40] V.G. Baryshevsky, V.V. Tikhomirov, Possibilities of obtaining polarized $e^+ e^-$ beams in proton accelerators, *Physics of Atomic Nuclei* **48** (1988) 429
- [41] V.V. Tikhomirov, Polarization effects accompanying penetration of high-energy electrons, positrons and gamma-quanta through crystals, *Rad. effects. and defects in solids.* **117** (1991) 27.
- [42] V.G. Baryshevsky, V.V. Haurylavets, M.V. Korjik, A.S. Lobko, V.A. Mechinsky, A.I. Sytov, V.V. Tikhomirov, V.V. Uglov, On the influence of crystal structure on the electromagnetic shower development in the lead tungstate crystals, *Nucl. Instrum. and Meth. B* **402** (2017) 35.
- [43] L. Bandiera, V.V. Tikhomirov, M. Romagnoni, N. Argiolas, E. Bagli, G. Ballerini, A. Berra, C. Brizzolani, R. Camattari, D. De Salvador, V. Haurylavets, V. Mascagna, A. Mazzolari, M. Prest, M. Soldani, A. Sytov and E. Vallazza, Strong reduction of the effective radiation length in an axially oriented scintillator crystal, *Phys. Rev. Lett.* **121** (2018) 021603.

- [44] V.G. Baryshevsky, A.A. Sokolsky, On the existence of the effect of oscillations of the polarization of a fast particle (channeling particle with a quadrupole moment), *Pis'ma Zh. Tekh. Fiz.* **6** (1980) 1419.
- [45] E. Bagli et. al., Electromagnetic dipole moments of charged baryons with bent crystals at the LHC, *Eur. Phys. J. C* **77** (2017) 828; Erratum *ibid.* **80** (2020) 680.
- [46] J. Fu, M.A. Giorgi, L. Henry, D. Marangotto, F. Martinez Vidal, A. Merli, N. Neri, and J. Ruiz Vidal, Novel method for the direct measurement of the tau lepton dipole moments, *Phys. Rev. Lett.* **123** (2019) 011801.
- [47] V. G. Baryshevsky, Electromagnetic dipole moments and time reversal violating interactions for high energy charged baryons in bent crystals at LHC, *Eur. Phys. J. C* **79** (2019) 350.
- [48] A.S. Fomin, A.Yu. Korchin, A. Stocchi, et al., Feasibility of measuring the magnetic dipole moments of the charm baryons at the LHC using bent crystals, *Journal of High Energy Physics*, **8**(2017)120, Aug 2017. [https://doi.org/ 10.1007/JHEP08\(2017\)120](https://doi.org/10.1007/JHEP08(2017)120).
- [49] N. Matsunami and L. M. Howe, A diffusion calculation of axial dechanneling in Si and Ge, *Radiation Effects*, **51** (1980) 111.
- [50] V.V. Tikhomirov, Quantum features of high energy particle incoherent scattering in crystals, *Phys. Rev. Accel. Beams.* **22** (2019) 054501; Erratum: *ibid.*, **23** (2020) 039901(E); arXiv: 2004.06020.
- [51] V.A. Bazylev, V.V. Goloviznin, Quantum theory of channeled electron and positron scattering in a crystal, *Zh. Eksp. Teor. Fiz.* **82** (1982) 1204; [*Sov. Phys. JETP* **55** (1982) 700].
- [52] V.A. Bazylev, S.B. Dabagov, Electromagnetic radiation under ncoherent and incoherent scattering of relativistic electrons in crystals, *Zh. Tekh. Fiz.* **58** (1988) 1563.
- [53] V.L. Ljuboshits, M.I. Podgoretsky, Multiple Coulomb scattering of ultrarelativistic charged particles moving at small angles to crystallographic planes, *Zh. Eksp. Teor. Fiz.* **87**, 717 (1984); [*Sov. Phys. JETP* **60** (1984) 409].
- [54] V.G. Baryshevsky, V.V. Tikhomirov, The role of incoherent scattering in radiation processes at small angles of incidence of particles on crystallographic axes or planes, *Zh. Eksp. Teor. Fiz.* **90**, 1908 (1986); [*Sov. Phys. JETP* **63** (1986) 1116].
- [55] V.V. Tikhomirov, Quantitative theory of channeling particle diffusion in transverse energy in the presence of nuclear scattering and direct evaluation of dechanneling length, *Eur. Phys. J. C.* **77** (2017) 483.

- [56] X. Artru, Quantum versus classical approach of dechanneling and incoherent electromagnetic processes in aligned crystals, 2020 JINST **15** (2020) C04010.
- [57] M.L. Ter-Mikaelian, Ultrafast electron scattering in crystals, Zh. Eksp. Teor. Fiz., **25** (1953) 289.
- [58] L. Bandiera, E. Bagli, G. Germogli, V. Guidi, A. Mazzolari, H. Backe, W. Lauth, A. Berra, D. Lietti, M. Prest, D. De Salvador, E. Vallazza, and V. Tikhomirov, Investigation of the electromagnetic radiation emitted by sub-GeV electrons in a bent crystal, Phys. Rev. Lett. **115** (2015) 025504.
- [59] A. Mazzolari, A. Sytov, L. Bandiera, G. Germogli, M. Romagnoni, E. Bagli, V. Guidi, V.V. Tikhomirov, D. De Salvador, S. Carturan, C. Durigello, G. Maggioni, M. Campostrini, A. Berra, V. Mascagna, M. Prest, E. Vallazza, W. Lauth, P. Klag, M. Tamisari, Broad angular anisotropy of multiple scattering in a Si crystal, Eur. Phys. J. C. **80** (2020) 63.
- [60] V.B. Berestetskii, E.M. Lifshitz, L.P. Pitaevskii (1982). Quantum Electrodynamics. Vol. 4 (2nd ed.). Butterworth Heinemann.
- [61] G. Moliere, Theorie der Streuung schneller geladener Teilchen II. Mehrfach und Vielfachstreuung, Z. Naturforsch., **3** (1948) 78.
- [62] H. Bethe, Moliere's theory of multiple scattering, Phys. Rev. **89** (1953) 1256.
- [63] U. Fano, Inelastic collisions and the Moliere theory of multiple scattering, Phys. Rev. **93** (1954) 117.
- [64] N. Bohr, The penetration of atomic particles through matter, Kgl. Dan. Vidensk. Selsk. Mat. Fys. Medd. **18** (1948) 8.
- [65] L.D. Landau, E.M. Lifshitz, Quantum Mechanics: Non-Relativistic Theory, Vol. 3 (3rd ed.) Pergamon Press, 1977.
- [66] L. D. Landau, E. M. Lifshitz, L. P. Pitaevskii (1984). Electrodynamics of Continuous Media. Vol. 8 (2nd ed.). Butterworth Heinemann.
- [67] A.M. Taratin and S.A. Vorobev, Proton volume capture in channeling regime in bent crystal, Zh. Tekh. Fiz. **55** (1985) 1598 [Sov. Phys. Tech. Phys. **30** (1985) 927].
- [68] Geant4. Overview. <http://geant4.web.cern.ch/>
- [69] W. Scandale, A.M. Taratin, Channeling and volume reflection of high-energy charged particles in short bent crystals. Crystal assisted collimation of the accelerator beam halo, Physics Reports, **815** (2019) 1.

- [70] H. A. Bethe, Intermediate Quantum Mechanics. Inc. New-York-Amsterdam: W.A. Benjamin, 1964.
- [71] J.D. Jackson, Classical Electrodynamics (3rd ed.). New York: John Wiley & Sons, 1999. ISBN 978-0-471-30932-1.
- [72] P. Sigmund, K.B. Winterborn, Small-angle multiple scattering of ions in the screening Coulomb region, Nucl. Instrum. and Methods, **119** (1974) 541.
- [73] M. Kitagawa, Y.H. Ohtsuki, Modified dechanneling theory and diffusion coefficients, Phys. Rev. B **8** (1973) 3117.
- [74] Y. H. Ohtsuki and H. Nitta, Theory of dechanneling. Relativistic Channeling, edited by R. Carrigan, Jr. and J. Ellison (Plenum, New York, 1987).
- [75] H. Nitta and Y. H. Ohtsuki, Dechanneling and stopping power of relativistic channeled particles, Phys. Rev., **B 38** (1988) 4404.
- [76] H. Esbensen, J. A. Golovchenko, Energy loss of fast channeled particles, Nucl. Phys., **A298** (1978) 382.
- [77] H. Esbensen et. al., Random and channeled energy losses in thin germanium and silicon crystals for positive and negative 2-15-GeV/c pions, kaons, and protons, Phys. Rev. B. **188** (1978) 1039.
- [78] A. F. Burenkov, F. F. Komarov, and M. A. Kumakhov, Energy loss of charged particles in crystals, Zh. Eksp. Teor. Fiz., **78**(1980)1474; [Sov. Phys. JETP **51** (1980) 741].
- [79] L.D. Landau, E.M. Lifshitz, The classical theory of fields, Vol. 2 (4rd ed.) Butterworth-Heinemann, 1994.
- [80] Review of Particle Physics Particle Data Group, P A Zyla et. al., Physics, Volume 2020, Issue 8, August 2020, 083C01, <https://doi.org/10.1093/ptep/ptaa104>
- [81] I. D. Feranchuk, L. I. Gurskii, L. I. Komarov, O. M. Lugovskaya, F. Burgazy, A. Ulyanenko, A new method for calculation of crystal susceptibilities for X-ray diffraction at arbitrary wavelength, Acta Cryst. **A58** (2002) 370.
- [82] O. D. Skoromnik, I. D. Feranchuk, A. U. Leonau, C. H. Keitel, Analytic model of a multi-electron atom, J. Phys. B: At. Mol. Opt. Phys. **50** (2017) 245007.
- [83] J. H. Hubbell et.al., Atomic form factors, incoherent scattering functions, and photon scattering cross sections, J. Phys. Chem. Ref. Data, **4** (1975) 471.